Oscillatory Vertical Coupling between a Whispering-Gallery Resonator and a Bus Waveguide

M. Ghulinyan,[1,*] F. Ramiro-Manzano,[2] N. Prtljaga,[2,†] R. Guider,[2,‡] I. Carusotto,[3] A. Pitanti,[4] G. Pucker,[1] and L. Pavesi[2]

[1]*Advanced Photonics and Photovoltaics Unit, Fondazione Bruno Kessler, I-38123 Povo, Italy*
[2]*Department of Physics, Nanoscience Laboratory, University of Trento, I-38123 Povo, Italy*
[3]*INO-CNR BEC Center and Department of Physics, University of Trento, I-38123 Povo, Italy*
[4]*NEST, Scuola Normale Superiore and Istituto Nanoscienze-CNR, Piazza San Silvestro 12, 56127 Pisa, Italy*
(Received 21 October 2011; revised manuscript received 8 January 2013; published 15 April 2013)

We report on a theoretical and experimental study of the optical coupling between a whispering-gallery type resonator and a waveguide lying on different planes. In contrast to the usual in-plane geometry, the present vertical one is characterized by an oscillatory behavior of the effective coupling as a function of the vertical gap. This behavior manifests itself as oscillations in both the resonance peak waveguide transmission and the mode quality factor. An analytical description based on coupled-mode theory and a two-port beam-splitter model of the waveguide-resonator vertical coupling is developed for arbitrary phase-matching conditions and is successfully used to interpret the experimental observations.

DOI: 10.1103/PhysRevLett.110.163901 PACS numbers: 42.25.Hz, 42.60.Da, 42.82.Gw

A typical strategy to study the physics of the planar whispering-gallery mode (WGM) resonators consists of exciting the cavity modes from an adjacent waveguide and collecting the transmitted light [1]. The resonator-waveguide coupling (RWC) takes place via an overlap of the evanescent fields of the waveguide and the resonator optical modes. In an *in-plane* geometry [Fig. 1(a)], where the waveguide and the resonator lay on the same plane, the mode coupling is known to grow exponentially when the gap x between these two is decreased. This behavior has important implications in the amplitude and the linewidth of resonant dips that appear in the waveguide transmission spectrum $T(\omega)$ at cavity mode frequencies. As the gap x is reduced, the cavity mode linewidth Γ increases monotonically. The transmission $T_{\rm dip}$ at resonance, in turn, vanishes at a single critical coupling gap x^* when the field propagating in the waveguide and the secondary emission by the resonator interfere destructively on exact resonance. This phenomenology is accurately captured by a theoretical model based on a spatially localized RWC [2,3] and is widely applied to all-integrated devices [4–7].

Besides, in present-day integrated optics a *vertical* coupling geometry for the RWC is also used. In this configuration, the resonator and the waveguide lay on different planes [Fig. 1(b)] [8–10]. Examples of technologies that opt for this approach are the heterogeneously integrated III-V resonators onto silicon waveguides [11,12], microelectromechanical systems [13], or doped silica glass-based resonators [8,14]. In contrast to lateral coupling, this approach does not require high-resolution lithography for the definition of narrow gaps and allows for an independent choice of materials and thicknesses for the optical components [8,9]. Advantageously, it permits us to realize the resonator and the waveguide in separate technological steps and, therefore, enables the engineering of an evanescent coupling of arbitrary strength [10]. Such features offer a larger design flexibility that can be of great utility in a number of applications to high-speed integrated optoelectronics as well as to cavity optomechanics.

So far, it has been assumed that the standard model of spatially localized RWC [3] should be able to describe accurately the RWC also in the vertical coupling geometry but no specific theoretical study has explicitly validated this assumption [15]. In this Letter we show both theoretically and experimentally that this common belief is actually wrong. In fact, in a vertical geometry, the effective gap L_v between the resonator and the waveguide remains

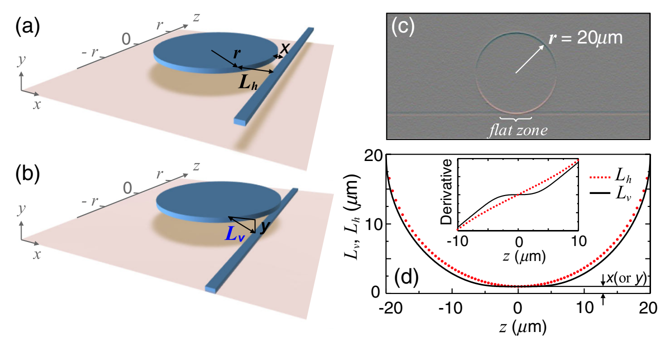

FIG. 1 (color online). (a),(b) Sketches of the in-plane (a) and the vertical (b) resonator-waveguide coupling geometries. (c) The digitally processed optical image of the vertically coupled resonator and the waveguide showing a relatively wide zone where the two are very close and almost parallel. (d) Plot of the resonator-waveguide separation as a function of the z coordinate along the waveguide axis in the in-plane [$L_h(z)$, red dotted line] and vertical geometries [$L_v(z)$, solid line]. The presence of the flat zone in $L_v(z)$ is highlighted in the inset, where the first derivative dL_v/dz is plotted. The curves are calculated for a 20 μm-radius resonator, minimum distance $x = 0.75$ μm for the in-plane case and $y = 0.75$ μm with lateral alignment $x = 0$ for the vertical coupling case.

almost constant over a sizable distance Λ along the waveguide axis z [Fig. 1(c)]. Within this *flat zone*, the waveguide and the resonator can be modeled as a pair of coupled parallel waveguides for which the coupled mode theory predicts a periodic exchange of optical power as a function of the propagation distance. In contrast to the monotonic exponential dependence of the effective RWC in the in-plane geometry, the vertical one is characterized by an oscillating effective coupling as a function of vertical gap y, with alternating under-and over-coupling regions, separated by several critical coupling points. Correspondingly, both the cavity mode linewidth Γ and the dip transmission $T_{\rm dip}$ show oscillating dependencies. An excellent qualitative agreement is found between the analytical model based on coupled mode theory and the experimental observations.

The crucial difference between the in-plane and the vertical coupling approaches is apparent from simple geometrical considerations. Let us first consider the in-plane geometry sketched in Fig. 1(a): in the waveguide and in the resonator, separated by a minimum gap of x, light propagates along the z axis and a circle of radius r, respectively. The local RWC depends exponentially on the physical distance between the waveguide and the resonator: it is nonzero in the $-r < z < r$ segment and varies as $L_h = x + r - \sqrt{r^2 - z^2}$ along the waveguide z axis. On the other hand, in the vertical geometry [Fig. 1(b)], the resonator and the waveguide modes propagate on different planes, separated by a vertical distance y. As a result, now the physical distance between the waveguide and the resonator depends on z as $L_v = (L_h^2 + y^2)^{1/2}$.

The difference between these two dependencies is illustrated graphically in Fig. 1(d). While $L_h(z)$ grows rapidly around its minimum at $z = 0$, $L_v(z)$ has a much smoother dependence over a wide region where it keeps an almost constant value. The extension Λ of the *flat zone* can be estimated from the position of the inflection points of dL_v/dz. A direct consequence of the flat zone is that the vertical geometry can be modeled to a good accuracy as a pair of parallel waveguides coupled via their evanescent fields: standard coupled-mode theory [16,17] can be then used to estimate the coupling coefficients starting from the physical parameters of the actual devices, such as the waveguide and resonator dimensions, their separation gap, and the material refractive indices.

An example of such a calculation is illustrated in Fig. 2. Panel (a) compares the length Λ of the flat zone to the half-period $L_c = \pi/2\gamma$ of the power exchange between the parallel waveguides as predicted by coupled mode theory. The wave vector of these longitudinal oscillations depends on the system parameters as $\gamma = [(\Delta\beta/2)^2 + C_{12}C_{21}]^{1/2}$, where $\Delta\beta = \beta_1 - \beta_2$ is the propagation constant mismatch between the two waveguides and C_{12} and C_{21} are the local mode overlap coefficients, which decrease exponentially with separation distance [2]. While the length Λ of the flat zone has a purely geometrical dependence on the resonator radius and the vertical gap [circles in Fig. 2(a)], the coupling length L_c (solid line) depends on both the geometry and the refractive indices of the waveguides and the coupling medium. As shown in the following, the interplay between these two will drive periodically the system into the critical coupling state. Under ideal phase-matching conditions $\Delta\beta = 0$, L_c depends exponentially on the gap y [dashed line in Fig. 2(a)]. For a phase mismatch $\Delta\beta \neq 0$, L_c saturates at large gaps to a finite value of $\pi/\Delta\beta$, but the energy exchange ceases to be complete, thus suppressing the coupling.

In order to evaluate the amplitude of the transmitted light through the waveguide after coupling to the resonator, we model the flat zone as a two-port beam splitter coupling the waveguide and the resonator modes [Fig. 2(b)]. Approximating them to be single mode waveguides and parallel at a constant distance within the flat zone, coupled mode theory relates the output field amplitudes a_{o1} and a_{o2} at the end of the flat zone to the incident ones a_{i1} and a_{i2} as

$$\begin{aligned} a_{o2} &= a_{i2}\exp\left(i\frac{\Delta\beta}{2}z\right)\left[\cos(\gamma z) - i\frac{\Delta\beta}{2\gamma}\sin(\gamma z)\right] \\ &\quad + a_{i1}\exp\left(i\frac{\Delta\beta}{2}z\right)\frac{C_{12}}{i\gamma}\sin(\gamma z), \\ a_{o1} &= a_{i1}\exp\left(-i\frac{\Delta\beta}{2}z\right)\left[\cos(\gamma z) + i\frac{\Delta\beta}{2\gamma}\sin(\gamma z)\right] \\ &\quad + a_{i2}\exp\left(-i\frac{\Delta\beta}{2}z\right)\frac{C_{21}}{i\gamma}\sin(\gamma z). \end{aligned} \tag{1}$$

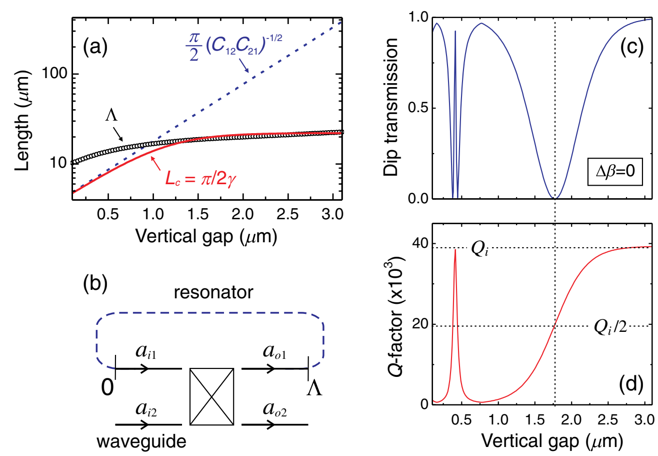

FIG. 2 (color online). (a) The calculated flat zone (circles) for a resonator of 40 μm diameter and the power transfer distance $\pi/2\gamma$ (solid red line) between parallel waveguides with refractive indices 1.963 and 1.825 and thicknesses of 400 and 250 nm, respectively. These result in a finite phase mismatch of $\Delta\beta = 0.142\ \mu\text{m}^{-1}$ at the operating wavelength of $\lambda = 1.58\ \mu$m. (b) Sketch of the two-port beam-splitter model. (c) The transmission $T_{\rm dip}$ and (d) the Q factor of the resonance as a function of the vertical coupling gap for the exact phase-matching $\Delta\beta = 0$ case. The intrinsic loss of the resonator is set to $\alpha = 0.9\ \mu\text{m}^{-1}$.

An explicit expression for the transmitted amplitude a_{o2} is found by solving the system of Eqs. (1) with the additional condition imposed by plane-wave propagation around the resonator,

$$a_{i1} = a_{o1} \exp\left[-i\frac{\omega n_1}{c}(2\pi r - \Lambda)\right]\exp[-\alpha L]. \quad (2)$$

Here, α is the overall intrinsic loss (material absorption, radiative, and surface scattering) of the resonator with a circumference of L and n_1 is the effective refractive index of the resonator mode. This last can be calculated by extracting the azimuthal mode number M of the mode and its frequency ω_0 from a numerical model (finite element method) and plugging them into the resonance condition $Mc/\omega_0 = n_1 r$.

After some mathematical transformations, for generic values of the phase matching parameter $\Delta\beta$, the transmission takes the form

$$T(\omega) = \left|\frac{a_{o2}}{a_{i2}}\right|^2 = \left|A - \frac{B}{e^{i(\omega n_1/c)L}e^{\alpha L} - A^*}\right|^2, \quad (3)$$

where $A = \exp(i\frac{\Delta\beta}{2}\Lambda)[\cos(\gamma\Lambda) - i\frac{\Delta\beta}{2\gamma}\sin(\gamma\Lambda)]$, $B = [C_{12}C_{21}/\gamma^2]\sin^2(\gamma\Lambda)$ and A^* is the complex conjugate of A. In particular, $T(\omega)$ shows a series of resonant dips each time the denominator in Eq. (3) reaches its minimum. By performing a series expansion of Eq. (3) in the vicinity of one of such resonances at ω_0, the waveguide transmission can be expressed in a Lorentzian form

$$T(\omega) \approx \left|A + i\frac{\frac{c}{n_1 L}Be^{-\alpha L}}{(\omega - \omega_0) - i\Gamma/2}\right|^2, \quad (4)$$

with an effective linewidth

$$\Gamma = \frac{2c}{n_1 L}(1 - e^{-\alpha L}|A|). \quad (5)$$

In a weak coupling regime, when $\gamma\Lambda \ll 1$, Γ tends to the intrinsic decay rate $\Gamma_i \simeq 2c\alpha/n_1$ (for relatively weak intrinsic loss, $\alpha L \ll 1$). The associated intrinsic (unloaded) Q factor of the cavity is therefore $Q_i = \omega_0\Gamma_i^{-1} = \frac{\omega_0 n_1}{2c\alpha}$. For stronger couplings, the decay rate displays oscillations as a function of $\gamma\Lambda$: for sufficiently low intrinsic losses, it periodically goes from the under- ($\Gamma < 2\Gamma_i$) to the over-coupling ($\Gamma > 2\Gamma_i$) regimes passing from the critical coupling ($\Gamma = 2\Gamma_i$) condition.

This physics is summarized in Figs. 2(c) and 2(d) for the exact phase-matching $\Delta\beta = 0$ case: the dip transmission T_{dip} at the resonance and its quality factor Q are plotted as a function of the vertical gap y. As the most significant features, we can mention the following: (i) the dip transmission T_{dip} shows huge oscillations as the gap y decreases. (ii) critical coupling ($T_{\mathrm{dip}} = 0$) occurs at distinctly different vertical gaps each time $\gamma(y)$ is such that the condition

$$\cos^2(\gamma\Lambda) + \left(\frac{\Delta\beta}{2\gamma}\right)^2\sin^2(\gamma\Lambda) = e^{-2\alpha L} \quad (6)$$

is fulfilled. Thanks to the sizable extension of the flat zone, the first critical coupling appears at a relatively large vertical gap of the order of 2 μm. (iii) starting from $Q \approx Q_i$ in the deep under-coupling regime for large gaps, the cavity Q shows huge oscillations from the under- to the over-coupling regime, and vice versa. Regions of the clear under-coupling regime $Q \approx Q_i$ are observed again for smaller gaps.

The physical origin of this rich behavior stems from the periodic exchange of optical energy between the waveguide and the resonator in the flat zone. These findings are contrasted with the in-plane case, where the spatially localized, pointlike nature of the RWC prevents oscillations from occurring: as the gap x is decreased, the Q factor is monotonically spoiled and critical coupling occurs at a single value of the gap only [2–7].

This theoretical model can be directly validated by comparing its predictions based on Eqs. (3)–(5) to experimental results. In our experiments, a large set of 40 μm-diameter SiN_x microdisk WGM resonators, coupled vertically to 1.8 μm-wide silicon oxynitride ($SiON_x$) waveguides were fabricated and characterized (see Ref. [9] for technical details). The bulk refractive indices of the two materials at a wavelength of 1.58 μm are 1.963 and 1.825, while the thicknesses are 400 and 250 nm for the resonator and the waveguide, respectively. This set of material and geometrical parameters leads to a slightly non-phase-matched situation with $\Delta\beta \approx 0.142\ \mu\mathrm{m}^{-1}$.

In Fig. 3 we show the experimental transmission spectrum of a device with a vertical gap of $y = 814$ nm over a 16 nm wavelength range. Here, two pairs of resonances,

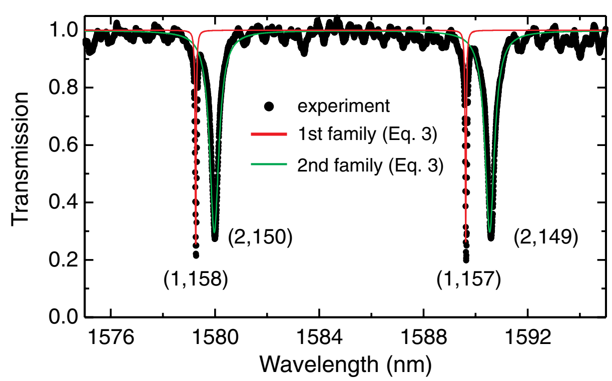

FIG. 3 (color online). Experimental transmission spectrum for a device with a nominal vertical gap $y = 814$ nm. Two series of narrow and broad resonances are visible, corresponding to modes of the first and of the second order radial families, respectively; for each resonant dip, the labels indicate the radial and the azimuthal quantum numbers of the corresponding mode. The experimental spectrum (dots) is compared to the theoretical prediction Eq. (3) for both first and second radial order mode families (solid lines).

corresponding to the first and second radial family modes, are present with markedly different linewidths.

The experimental transmission spectrum is compared to the theoretical one predicted by Eq. (3) using the value of the flat zone length Λ corresponding to the nominal 814 nm gap. The comparison shows a good agreement with the experiment in terms of both the free spectral range, the minimum transmission T_{dip} and the quality factor Q of the resonance: estimates for these two latter quantities are extracted by a Lorentzian fit to the experimental spectrum once the background of the broader peak has been subtracted out.

The higher order modes of the resonator can also be described using the same Eqs. (3)–(5) by considering the effective refractive index n_i and the propagation constant β_i of the ith radial order mode. As an example, in Fig. 3 we show also the $T(\omega)$ curve for the second radial mode family. A detailed analysis of higher order modes is out of the scope of the present study, therefore, here we concentrate our attention on the narrow resonances only.

To get a clear picture of the physics of the vertical coupling, we study the dependence of the dip transmission T_{dip} and the Q factor as a function of the vertical gap y. For each value of y, the experimental T_{dip} and the Q of the first family resonance at around $\lambda \approx 1.58$ μm were extracted from an individual device (waveguide + resonator) with that nominal value of the vertical gap y [18]. These results are summarized in Figs. 4(a) and 4(b). In spite of the experimental uncertainties, the validity of the standard model with a pointlike in-plane coupling [2,3] is clearly disproved [see the best-fit T and Q dotted curves in Figs. 4(a) and 4(b)]: as the gap is reduced from around 1.25 μm to around 800 nm, the quality factor Q increases again by a factor of almost three. Another feature in stark disagreement with the standard model is the presence of two distinct values of the vertical gap $y \simeq 640$ nm and $y \simeq 885$ nm at which critical coupling occurs. For vertical gaps in between these two higher resonant transmission states are observed again; we measured a T_{dip} as high as 60% at a vertical gap of 730 nm. From the experimental value Q_{cc} of the quality factor at critical coupling we extract an intrinsic $Q_i = 2Q_{cc} \approx 4 \times 10^4$. This shows that the points for the largest values of the vertical gap are already in the over-coupling regime.

These results are further illustrated in the right panels of Fig. 4, where experimental transmission spectra at a few selected coupling gaps 1470, 1260, 885, and 695 nm are shown, corresponding to the A, B, C, D labels in panels (a) and (b). Starting from the largest gap already well in the over-coupling regime (A), the resonance penetrates further into the over-coupling regime for a smaller gap (B). When the gap is decreased even further, it shows first a critical coupling regime (C) and finally enters into an under-coupling regime (D).

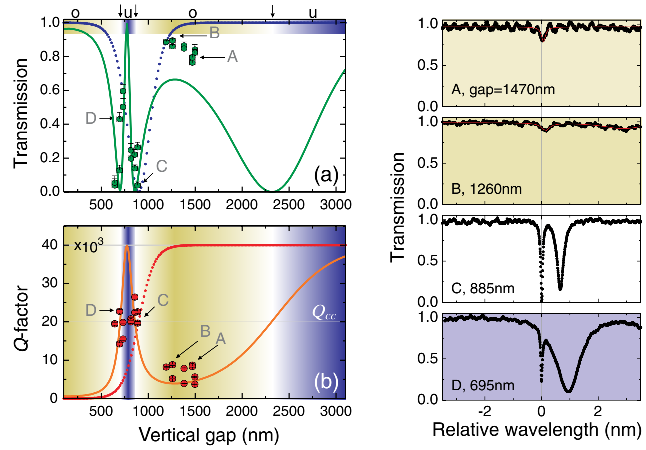

FIG. 4 (color online). Vertical gap dependence of the resonant transmission T_{dip} (a) and the resonance Q factor (b) for the mode of the wavelength closest to 1.58 μm. Experimental points are compared to the theoretical predictions of [Eqs. (4) and (5)] (solid line). For comparison, the T and Q trends for the point coupling model are reported as dotted lines. The background colors underline the regions where undercoupling (blue, u), critical coupling (white, ↓), and overcoupling (yellow, o) are expected. The right panels show the experimental spectra around $\lambda = 1.58$ μm for a few specific values of the gap as indicated in the left panels by the A, B, C, D labels: the x-axis zero is set to the center of the resonance dip.

Using the value for $\alpha \approx 0.9$ $\mu\mathrm{m}^{-1}$, extracted from the experimental Q_i, and inserting the nominal parameters (geometrical dimensions of the resonator and the waveguide and material indices) of the actual devices, we have calculated the theoretical curves for $T_{\mathrm{dip}}(y)$ and $Q(y)$. These are plotted as solid lines in Figs. 4(a) and 4(b), showing a marked oscillatory behavior in qualitative agreement with experimental data. Even though for a more quantitative comparison a sophisticated theoretical model is required, the available experimental data give already unambiguous indications in favor of the spatially extended RWC theory developed in this Letter.

To conclude, in this Letter we have theoretically and experimentally demonstrated radically new behaviors that occur when a whispering-gallery microresonator is coupled to a waveguide lying on a different plane. In this vertical coupling geometry, the effective coupling between the waveguide and the resonator does not increase monotonically as the gap is reduced, but shows huge oscillations between the under- and over-coupling regimes. The dramatic differences between the vertical and the in-plane coupling geometries have wide consequences to optical circuits and their applications to fundamental science [19] and technological applications [12,14]. For instance, the use of vertical coupling geometry in second-harmonic generation experiments will allow to freely tune the Q factor of the second-harmonic mode at 2ω while keeping the pump at the fundamental frequency ω in critical coupling. Also, cavity optomechanics experiment will benefit of the possibility of maintaining high values of the cavity Q factor in spite of the coupling gap variations due to the mechanical vibrations of the resonator.

The authors thank M. R. Vanacharla for stimulating discussions, and MTLab-FBK staff for the support in realizing samples. This work has been supported by NAoMI-FUPAT. F. R. M. thanks the project APPCOPTOR financed through an FP7 EU Marie Curie fellowship.

*ghulinyan@fbk.eu

†Present address: Department of Physics and Astronomy, University of Sheffield, S3 7RH Sheffield, United Kingdom.

‡Present address: Institute of Semiconductor and Solid State Physics, Johannes Kepler Universität, Altenbergerstrasse 69, A-4040 Linz, Austria.

[1] *Practical Applications of Microresonators in Optics and Photonics*, edited by A. B. Matsko (CRC Press, New York, 2009).

[2] A. Yariv, Electron. Lett. **36**, 321 (2000).

[3] S. M. Spillane, T. J. Kippenberg, O. J. Painter, and K. J. Vahala, Phys. Rev. Lett. **91**, 043902 (2003).

[4] J. Niehusmann, A. Vörckel, P. H. Bolivar, T. Wahlbrink, W. Henschel, and H. Kurz, Opt. Lett. **29**, 2861 (2004).

[5] M.-C. M. Lee and M. C. Wu, IEEE Photonics Technol. Lett. **17**, 1034 (2005).

[6] M. Soltani, S. Yegnanarayanan, and A. Adibi, Opt. Express **15**, 4694 (2007).

[7] K. Preston, P. Dong, B. Schmidt, and M. Lipson, Appl. Phys. Lett. **92**, 151104 (2008).

[8] B. E. Little, S. T. Chu, W. Pan, D. Ripin, T. Kaneko, Y. Kokubun, and E. Ippen, IEEE Photonics Technol. Lett. **11**, 215 (1999).

[9] M. Ghulinyan, R. Guider, G. Pucker, and L. Pavesi, IEEE Photonics Technol. Lett. **23**, 1166 (2011).

[10] F. Ramiro-Manzano, N. Prtljaga, L. Pavesi, G. Pucker, and M. Ghulinyan, Opt. Express **20**, 22934 (2012).

[11] J. Van Campenhout, P. Rojo Romeo, P. Regreny, C. Seassal, D. Van Thourhout, S. Verstuyft, L. Di Cioccio, J.-M. Fedeli, C. Lagahe, and R. Baets, Opt. Express **15**, 6744 (2007).

[12] L. Liu *et al.*, Nat. Photonics **4**, 182 (2010).

[13] M.-C. M. Lee and M. C. Wu, Opt. Express **14**, 4703 (2006).

[14] M. Ferrera, L. Razzari, D. Duchesne, R. Morandotti, Z. Yang, M. Liscidini, J. E. Sipe, S. Chu, B. E. Little, and D. J. Moss, Nat. Photonics **2**, 737 (2008).

[15] The lateral alignment of a vertically coupled resonator and a waveguide have been studied by R. Stoffer, K. R. Hiremath, M. Hammer, L. Prkna, and J. Čtyroký, Opt. Commun. **256**, 46 (2005); The optimization of the coupling efficiency as a function of lateral in-plane alignment under fixed vertical gap conditions has been addressed by F. Mandorlo, P. Rojo Romeo, X. Letartre, R. Orobtchouk, and P. Viktorovitch, Opt. Express **18**, 19 612 (2010).

[16] D. L. Lee, *Electromagnetic Principles of Integrated Optics* (Wiley, New York, 1986).

[17] H. A. Haus and W. P. Huang, Proc. IEEE **79**, 1505 (1991); W.-P. Huang, J. Opt. Soc. Am. A **11**, 963 (1994).

[18] The y-gap value has been extracted from interferometric measurements and has an accuracy of ± 30 nm. The vertical error bars for $T_{\rm dip}(y)$ reflect the uncertainty of the definition of the 100% waveguide transmission level which can be masked by the Fabry-Perot fringes, originating from waveguide facet reflections. The error bars of the experimental Q data were obtained from the error of Lorentzian linewidths. Statistically, the linewidth errors are larger for broad and shallow (overcoupled) resonances due to the non-negligible Fabry-Perot oscillations within the cavity resonance.

[19] M. Hafezi, E. Demler, M. Lukin, and J. Taylor, Nat. Phys. **7**, 907 (2011).